*Early Disk-Galaxy Formation from JWST to the Milky Way*
*Proceedings IAU Symposium No. 377, 2024*
*F. Tabatabaei, B. Barbuy & Y.-S. Ting, eds.*
doi:10.1017/S1743921323001163

# What the JWST can tell us about the Origin of Multiple Stellar Populations in Globular Clusters

**Anna F. Marino**

Istituto Nazionale di Astrofisica - Osservatorio Astronomico di Padova, Vicolo dell'Osservatorio 5, Padova, IT-35122
Istituto Nazionale di Astrofisica - Osservatorio Astrofisico di Arcetri, Largo Enrico Fermi, 5, Firenze, IT-50125. email: anna.marino@inaf.it

**Abstract.** I present the first results of multiple stellar populations in globular clusters from James Webb Space Telescope (JWST) data. We obtained combined NIRSpec and NIRCam data of the GC 47 Tucanae to investigate the properties of the different stellar populations in the low-mass regime, down to $\sim$0.5 $M_{\odot}$. Our analysis of both the photometric data and the spectra suggests that the multiple stellar populations among M dwarfs share similar properties of those extensively studied on bright red giant branch stars. The comparison between stellar populations' properties at different stellar mass, e.g. at the red giants and M dwarfs' phases, can potentially provide strong constraints to the formation scenarios of the still eluding phenomenon of the multiple populations in star clusters.

**Keywords.** globular clusters: general, stars: population II, stars: abundances, techniques: photometry, techniques: spectroscopy.

## 1. Introduction

Globular clusters (GCs) have always been among the most intensively studied stellar systems, however, we have never really understood how they formed at high-z. With the presence of more than one stellar population in these ancient stellar aggregates, answering these questions became harder than ever (e.g. Renzini et al. 2015; Milone & Marino 2022).

Most of the exploration of the multipe stellar population phenomenon is based on the exploitation of the UV region of the spectrum. To now, the best tool to investigate the properties of the different populations of stars is indeed by means of the nicknamed "Chromosome Map" diagrams (ChM), which exploit UV multi-band photometry to maximise the separation of stellar populations on a plane mostly sensitive to light elements (Milone et al. 2015, 2017; Marino et al. 2019a).

The James Webb Space Telescope (JWST) opens the observation window to the mid-infrared domain, which is still poorly explored in the context of multiple populations. Pioneering analysis of M dwarfs in GCs, conducted by coupling *HST* IR images with spectral synthesis performed with the chemical abundances of 1P and 2P stars, has demonstrated that the properties of the multiple populations can be inferred in stars with mass as low as $\lesssim$0.5 $M_{\odot}$ (e.g. Milone et al. 2014; Dotter et al. 2015; Milone et al. 2019; Dondoglio et al. 2022). The JWST will be able to observe the faint M dwarf stars in GCs quite efficiently providing us with the possibility of really constraining the properties of multiple populations in a large stellar mass range, and getting crucial insights into their origin.

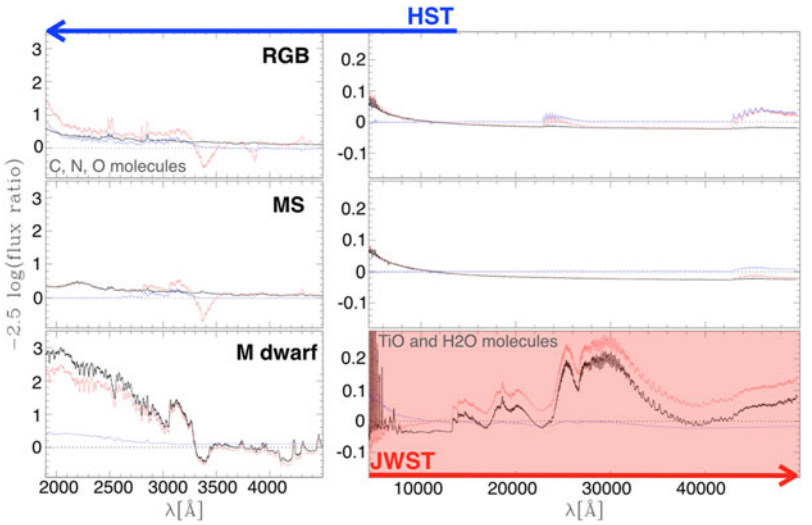


**Figure 1.** The black lines compare the fluxes of simulated spectra for stars with similar magnitude but 1P-like and 2P-like stellar compositions, with 2P stars being enhanced in helium and nitrogen, and depleted in carbon and oxygen with respect to the 1P. From top to the bottom we represent the case of one RGB, MS and M dwarf star. The pink lines refer to stars with the same He content abundances as 1P stars but different abundances of C, N, and O, while the azure lines are derived from spectra with the same C, N, and O content as 1P stars but enhanced helium content. Note the different scale for the left and right panels.

So far, two competing scenarios are available to account for the presence of multiple stellar populations in GCs: 1) multiple bursts of star formation (e.g. Decressin et al. 2007; de Mink et al. 2009; Ventura & D'Antona 2009; Denissenkov & Hartwick 2014; Renzini et al. 2022); 2) accretion of material onto existing stars (e.g. Bastian et al. 2013; Gieles et al. 2018). In the first scenario the population pattern is expected to be identical for stars with different masses, while the accretion scenario should result in substantially more pronounced chemical differences and fractions of second population stars at higher-masses. Multiple stellar populations in the M dwarf regime, down to ∼0.5 $M_{\odot}$, may indeed provide the key to understand the formation mechanisms of this phenomenon allowing us to disentangle between different scenarios.

## 2. A theoretical background

To set best strategies to investigate multiple stellar populations in GCs, we started by analysing how stars with different chemical abundances distribute on photometric diagrams constructed by exploiting the filters available for NIRCam on board of the JWST. In Figure 1 we illustrate flux ratios obtained by comparing synthetic spectra with typical chemical composition as those observed in Milky Way GCs. Specifically, synthetic spectra have been computed by using ATLAS and SYNTHE programs† by varying chemical abundances for C, N, O, and by assuming stellar structural parameters consistent with different helium content.

An inspection of the flux ratios represented in Figure 1 clearly suggests that, while the UV region is very efficient in disentangling stars with the distinct chemical composition of different stellar populations for all the stars from the M dwarfs to the RGBs, the mid-IR range available for NIRCam, is able to efficiently separate stars only on the low-mass

† http://kurucz.harvard.edu

https://doi.org/10.1017/S1743921323001163 Published online by Cambridge University Press

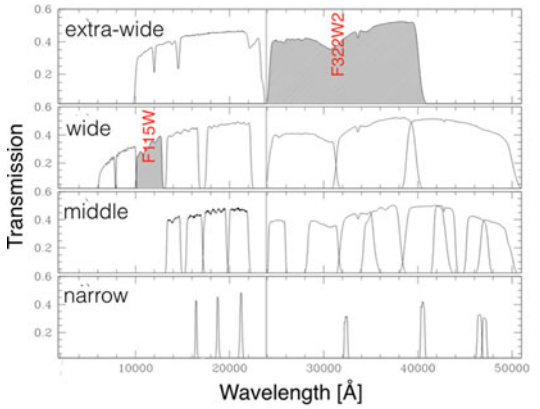


| Y | 0.25 | 0.33 | 0.33 | 0.25 |
|---|---|---|---|---|
| [C/Fe] | +0.0 | +0.0 | ↓ | ↓ |
| [N/Fe] | +0.0 | +0.0 | ↑ | ↑ |
| [O/Fe] | +0.4 | +0.4 | ↓ | ↓ |

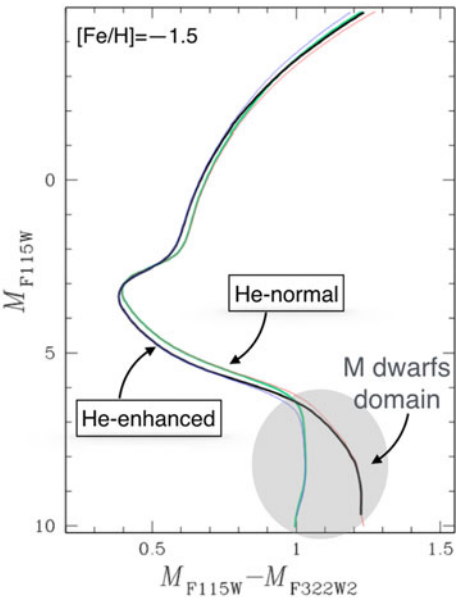


**Figure 2.** Stellar isochrones with a metallicity of [M/H]=−1.5 constructed by assuming the chemical abundance variations typically observed among the different stellar populations in GCs. The displayed isochrones are in a plane constructed by using magnitudes in the wide and extra-wide filters F115W and F322W2 (see upper-left panel). The chemical abundance pattern for isochrones represented with different colors is schematically listed in the table on the lower-left panel: green and blue are used for reference C, N, O abundances, while black and red have C, N, O abundances varyed as observed in the 2P stars, e.g. C and O-depleted, N-enhanced; the green and red isochrones have standard He, while the blue and black ones are He-enhanced. The expected CMD from the combination of these filters is the one that more efficiently separates the different stellar populations in the M dwarf regime (Milone et al. 2023).

regime of M dwarfs. The species responsible for this separation are mostly the $H_2O$ and the TiO molecules.

As a further step, we constructed isochrones that take into account the considered chemical abundance changes in the atomosphere, and inspect all the combinations from the NIRCam filters, including the extra-wide, wide, middle and narrow ones (see upper-left panel in Figure 2). To this aim we used isochrones from the Dartmouth stellar evolution database (Dotter et al. 2008) to which we applied our synthetic spectra to account for the variations in the atmosphere.

The color that more efficiently separates the multiple populations along the M dwarf sequence, below the main sequence knee, is $M_{F115W} - M_{F322W2}$. In Figure 2 we show the corresponding isochrones in the $M_{F115W}$ vs. $M_{F115W} - M_{F322W2}$ plane. Specifically, isochrones with variations in He (but the same C, N, O) and conversely, with variations in the C, N, O abundances (but the same He) have been plotted. These isochrones suggest that stellar populations with different He, from the standard value of $Y$=0.25 to $Y$=0.33, can be distinguished along the upper MS and the fainter RGB. However, at below the MS knee, isochones with different He overlap each other, while two sequences corresponding to different abundances of C, N, and O significanlty diverge towards fainter magnitudes.

We conclude that the JWST will be efficient in the analysis of the multiple stellar population phenomenon in the low-mass regime of the M dwarfs. As discussed in Section 1, the analysis of these stars is crucial to constrain the *real nature* of the multiple stellar populations in GCs.

https://doi.org/10.1017/S1743921323001163 Published online by Cambridge University Press

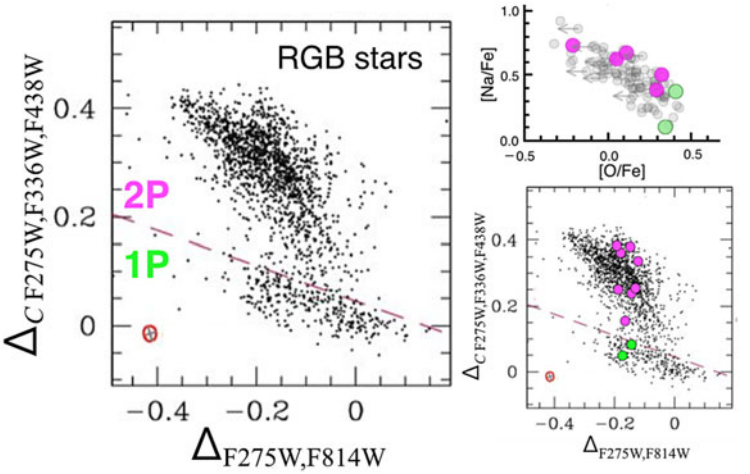


**Figure 3.** Chromosome map of red giant branch stars in the GC 47 Tucanae (Milone et al. 2017). The red dashed line on the left panel separates 1P from 2P stars. The typical observational error is represented in the bottom-left corner. The Na-O anticorrelation for this GC is shown on the right-upper panel by using chemical abundances from Carretta et al. (2009). 1P and 2P stars, shown in green and magenta, respectively, are distributed on different regions of the Na-O plane (Marino et al. 2019a).

## 3. Our target: 47 Tucanae

The GC 47 Tucanae is one of the most investigated in the Milky Way, both in terms of chemical abundances from spectroscopy, and in terms of photometric diagrams. As shown in Figure 3, this GC clearly displays a 1P and 2P on the ChM (Milone et al. 2017). As observed for the Milky Way GCs, stars with different light element abundances, e.g. O and Na, have a different location on the ChM photometric diagram (right panels in Figure 3): stars similar to the Halo field stars, enhanced in O, are distributed on the 1P, while stars depleted in O and enhanced in Na occupy the upper part of the ChM, i.e. the 2P region (Marino et al. 2019a).

The observed extended 1P on the $x$ axis of the ChM is not consistent with a simple stellar population Milone et al. (2017). This intriguing feature has been observed in most GCs with an available ChM, and, as first suggested by Milone et al. (2015), could be qualitatively consistent either with an internal variation in He and/or in the overall metallicity. Spectroscopic analysis based on high-resolution data on NGC 3201 favours the presence of small variations in metals among 1P stars (Marino et al. 2019b). The existence of metallicity variations is also corroborated by recent photometric investigation by Legnardi et al. (2022).

We recently obtained UVES high-resolution spectra to analyse metallicity among the 1P of 47 Tucanae. As shown in Figure 4, our chemical abundances suggest that the 1P stars of this GC are consistent with a small variation in metals by ∼0.10 dex (Marino et al. 2023a). An inhomogeneity in metallicity for 1P stars, hence with similar abundances of light elements, could enlighten us about the properties of the molecular clouds where GCs originated at high-z and constrain star-formation in the primordial Universe.

## 4. Results

By keeping in mind what discussed in Section 2, we obtained NIRSpec spectra and NIRCam images for 47 Tucanae, that optimize the detection of multiple stellar populations in GCs (GO2560; PI: Marino). We gathered NIRSpec spectra by using the

https://doi.org/10.1017/S1743921323001163 Published online by Cambridge University Press

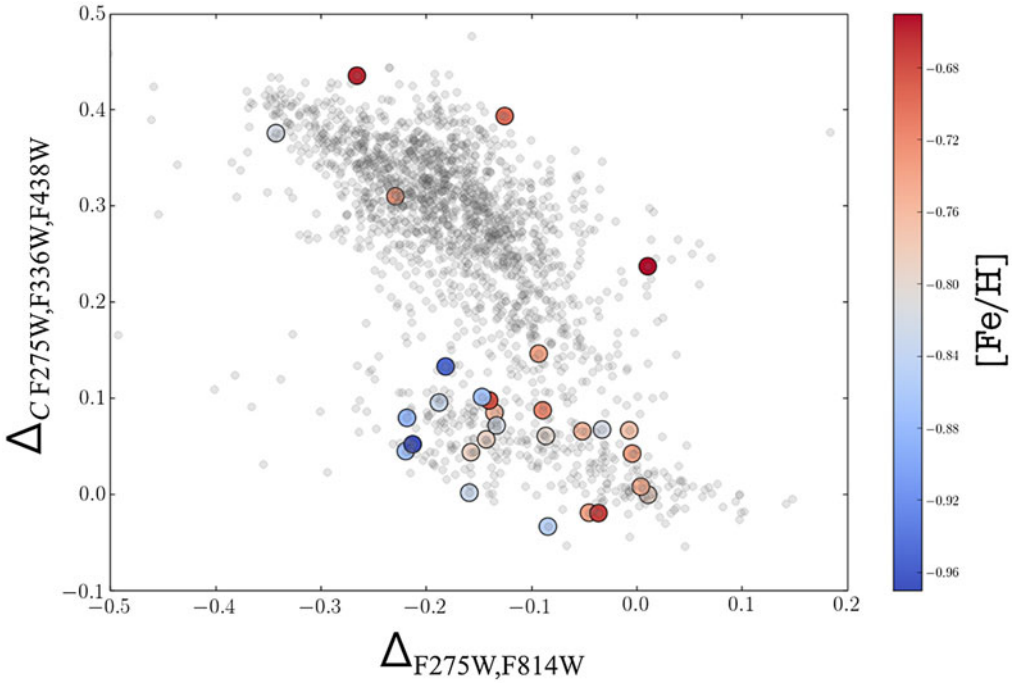


**Figure 4.** Chromosome map of red giant branch stars in the GC 47 Tucanae, with superimposed stars with available FLAMES-UVES spectra. The color of the spectroscopic targets is indicative of the inferred iron chemical abundance, as indicated by the column bar on the right (Marino et al. 2023a).

G235M/F170LP disperser-filter combination which provides a range in wavelength of 1.66-3.07 $\mu$m and a resolution of R$\sim$1000. Parallel observations with NIRCam observed in the two filters F115W and F322W2, those that most efficiently ensure the separation of multiple among M dwarfs.

Unfortunately, our observations experienced technical issues. Specifically wind-tilt events affecting some of the images, and problems with the nodding that resulted in missing spectra in one of the two nod positions. These issues did not provide the expected S/N and new observations have been planned in June.

Starting from the NIRCam images, a CMD obtained from our observations is shown in Fig. 5 (Milone et al. 2023). The 47 Tucanae stars, in the box, clearly separate from the Small Magellanic Cloud, whose stars distribute on the bluer side. For the GC stars, the $m_{\rm F115W} - m_{\rm F322W2}$ color is broaden, beyond the observational errors. The color broadening dramatically increases below the MS knee, in the domain of M-dwarfs. For a fixed F115W mag, the majority of MS M-dwarfs show blue colors, with a tail of stars distributed towards the red. Intriguingly, at fainter magnitudes ($m_{\rm F115W} \gtrsim$24) we observe a narrow tail of stars, mostly connected with the blue part of the M dwarf MS. These stars may be tentatively associated with stars with masses smaller than $\sim$0.1 M$_\odot$ (e.g. D'Antona & Mazzitelli 1994; Milone et al. 2012; Baraffe et al. 2015). In this case, it would be the first observational detection of such stars in a GC CMD.

Figure 6 shows isochrones with different content of He ($Y$), C, N, O, and Fe, in the $M_{\rm F115W}$ vs. $M_{\rm F115W} - M_{\rm F322W2}$ plane, constructed by assuming the two NIRCam filters exploited for our observations. A list of the used chemical abundances is displayed in the table on the right side. We verified that, by adding the third filter F606W from *HST* it is possible to separate multiple stellar populations on a pseudo-color-color diagram, as

https://doi.org/10.1017/S1743921323001163 Published online by Cambridge University Press

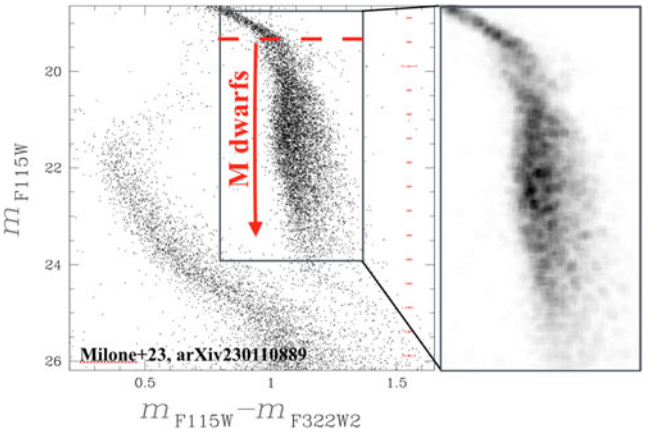


**Figure 5.** JWST CMD $m_{\rm F115W}$ vs. $m_{\rm F115W} - m_{\rm F322W2}$ of 47 Tucanae from Milone et al. (2023). On the left side we show the complete photometry for the observed field of view, which also includes the Small Magellanic Cloud on the bluer side. An zoom of the 47 Tucanae CMD is shown on the right panel as an Hess diagram. The color broadening below the MS knee, in the M dwarf domain, is clear.

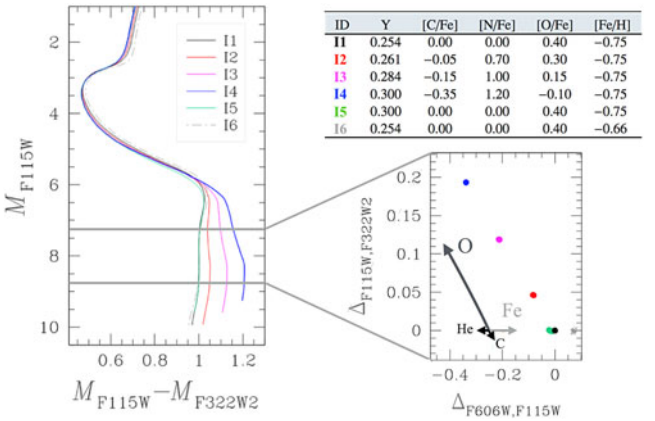


| ID | Y | [C/Fe] | [N/Fe] | [O/Fe] | [Fe/H] |
|---|---|---|---|---|---|
| I1 | 0.254 | 0.00 | 0.00 | 0.40 | −0.75 |
| I2 | 0.261 | −0.05 | 0.70 | 0.30 | −0.75 |
| I3 | 0.284 | −0.15 | 1.00 | 0.15 | −0.75 |
| I4 | 0.300 | −0.35 | 1.20 | −0.10 | −0.75 |
| I5 | 0.300 | 0.00 | 0.00 | 0.40 | −0.75 |
| I6 | 0.254 | 0.00 | 0.00 | 0.40 | −0.66 |

**Figure 6.** Isochrones in the $M_{\rm F115W}$ vs. $M_{\rm F115W} - M_{\rm F322W2}$ plane, constructed by assuming the different chemical abundances listed in the upper-right table (see Section 2) (Milone et al. 2023). By considering points in the mag interval within the two grey lines, a theoretical ChM has been obtained by adding to the two JWST filters F115W and F322W2, a third filter from the *HST*, namely F606W. The impact size of each considered abundance on the ChM is displayed by the length of the arrows. The chemical specie that most changes the location of a star in this plane is oxygen (note that the direction of the O abundance depletion is opposite to the arrow, being more O-depleted stars on the upper part of the diagram).

displayed on the bottom-right panel. This theoretical diagram has been obtained for the points in the indicated mag interval corresponding to the M dwarf domain, and represents an efficient ChM for M dwarfs in GCs.

The M dwarfs ChM is mostly sensitive to oxygen. Stars with chemical abundances consistent with the 1P are distributed on the lower part of this theoretical plane. While O-depleted stars locate on higher and higher values of $\Delta_{\rm F115W,F322W2}$, increasing the metallicity by ∼0.10 dex moves a star to larger values of $\Delta_{\rm F606W,F115W}$ on the $x$ axis. Helium and carbon have smaller impact on this plane.

https://doi.org/10.1017/S1743921323001163 Published online by Cambridge University Press

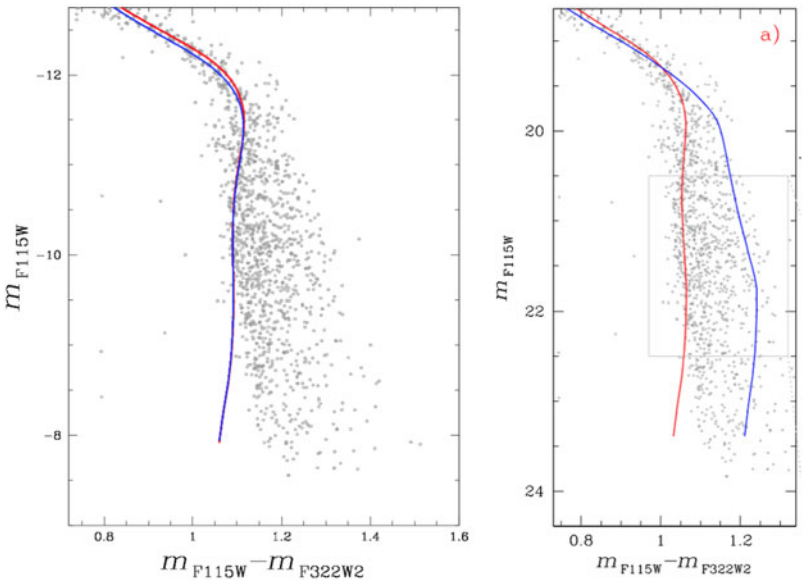


**Figure 7.** JWST CMD of 47 Tucanae with super-imposed isochrones with the same O abundances (left panel) and with [O/Fe] varied by 0.4 (right panel).

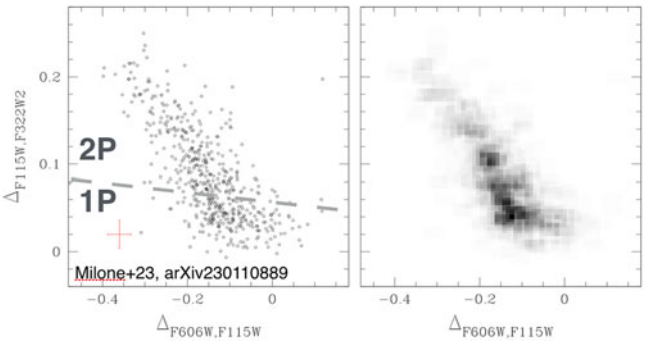


**Figure 8.** ChM from combined JWST-*HST* observations of 47 Tucanae M dwarfs (Milone et al. 2023). On the left panel the dashed line separates 1P from 2P stars. The right panel is the Hess diagram of the ChM. The expected error is represented in red on the left-side panel.

By using these isochrones to interpret our CMD from JWST observations, it is clear that isochrones with the same O, and different He, do not fit the CMD (see Figure 7). Instead, by decreasing O by 0.40 dex the $m_{F115W} - m_{F322W2}$ color became sensibly redder, and it is possible to qualitatively reproduce the observed spread in color of M dwarfs. This in turn suggests that the variation in O of M dwarfs is similar to the one observed on the red giants.

The same conclusions can be made from the ChM constructed by exploiting the available F606W filter from *HST* (see Figure 8). Similarly to the RGB, it is possible to identify different stellar populations on the ChM of the lower mass stars: a 1P distributes on the lower side of the map, while 2P stars have higher values along the $y$ axis, with most of them having $\Delta_{F115W,F322W2} \lesssim 0.12$. A remarkable difference between this ChM and the RGB one (shown in Figure 3) is that for the M dwarfs it does not look to exist a clear separation between 1P and 2P stars, as happens instead in RGB stars. This difference is

https://doi.org/10.1017/S1743921323001163 Published online by Cambridge University Press

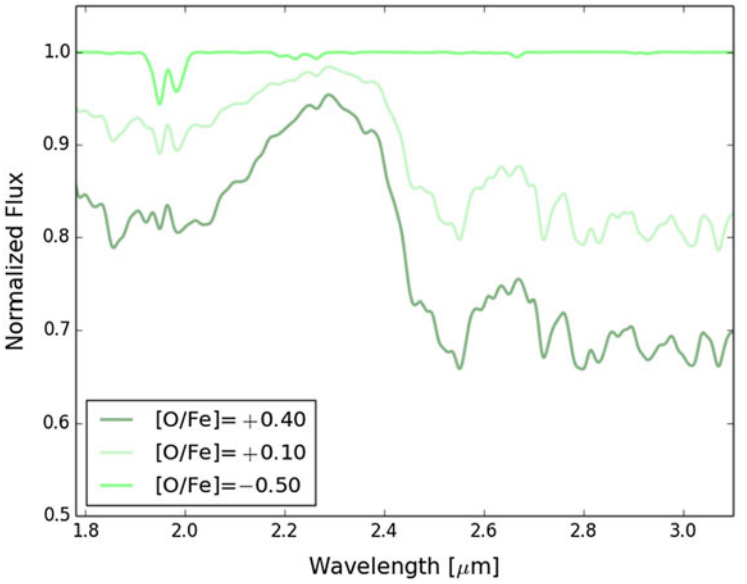


**Figure 9.** Simulated spectra of M dwarfs at the metallicity of 47 Tucanae. The spectra have been computed by varying oxygen abundances and keeping constant all the other chemical species. Oxygen abundances have been varyed by the amounts typically observed in Milky Way GCs.

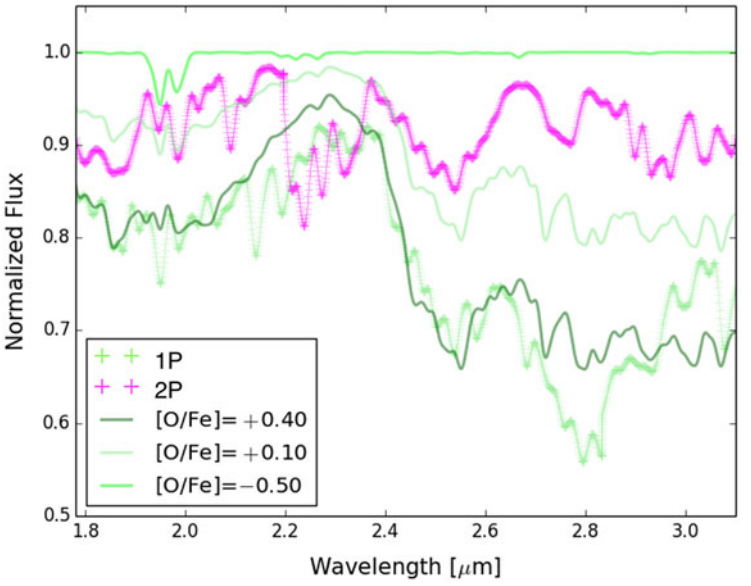


**Figure 10.** Two observed NIRSpec spectra of 47 Tucanae M dwarfs. Green and magenta crosses represent a 1P and 2P M dwarf, respectively. Super-imposed to the observed spectra are three spectra simulated at [O/Fe]=−0.50,+0.10,+0.40 dex.

https://doi.org/10.1017/S1743921323001163 Published online by Cambridge University Press

likely related to the fact that the RGB ChM is mostly sensitive to nitrogen, and might indicate a different evolution in the two chemical species.

Noticeably, the range of 1P M dwarfs on the $\Delta_{\rm F606W,F115W}$ is large, not consistent with a homogeneous stellar population. As discussed in Section 3, an inhomogeneity among the 1P on the ChM has been observed also in red giants, and high-precision spectroscopy favours an internal variation in metals for these stars (Marino et al. 2023a). As dispayed in Figure 6, expectations on the theoretical $\Delta_{\rm F115W,F322W2}$ vs. $\Delta_{\rm F606W,F115W}$ plane suggest that the values of $\Delta_{\rm F606W,F115W}$ are mostly affected by variations in metals for M dwarfs. This is consistent with what observed for red giants, and further suggests a primordial inhomogeneity in the molecular cloud from which 47 Tucanae formed.

Simulated spectra in the wavelength range of our NIRSpec data suggest that abundances of oxygen are those that mostly affect the shape of the M dwarfs spectra through the $H_2O$ molecules. Figure 9 shows three simulated spectra of M dwarfs with varied O abundances. Typical Halo field stars, enhanced in O, are deeply absorbed at these wavelengths. Decreasing oxygen, the spectrumm is less and less absorbed up to being almost flat for extremely-low O abundances ([O/Fe]$= -0.5$ dex). Similar simulations suggest that these spectra are instead marginally affected by carbon variations, while nitrogen does not impact at all.

Two observed NIRSpec spectra are represented in Figure 10. Specifically, two M dwarfs with similar atmospheric parameters, but belonging to the 1P and 2P populations have been represented. Comparing simulated spectra with observed ones immediately suggests that M dwarf spectra are very differently absorbed. They span a large range in oxygen, from [O/Fe]$\sim$0.10 dex to $\sim$0.4 dex.

## 5. Conclusions

Our pioneriing analysis of multiple stellar populations from JWST demonstrates the efficience of this telescope in the analysis of the M dwarfs, giving us the opportunity to investigate the phenomenon in a poorly-explored low stellar mass regime. The anaysed NIRCam images have allowed us to construct the deepest CMD, so far, with evidence of multiple stellar populations revealed in a GC, and the possible detection of very low-mass stars. Surely, many others will come soon thanks to new JWST observations.

This investigation outlines how the JWST data for M dwarfs are extremely sensitive to the internal variations in oxygen, via the interplay of molecules involving O, primarily $H_2O$ molecules. The existence of the typical variations among stellar populations in O, as observed on the red giants, gives the opportunity to distinguish different stellar populations in the M dwarfs' domain.

NIRCam images in F115W and F322W2, coupled with the *HST* filter F606W, have allowed us to construct a ChM of M dwarfs, where we clearly observe multiple stellar populations and an extended 1P, similarly to what observed on the ChM of red giant branch stars. The comparison of the $m_{\rm F115W}$ vs. $m_{\rm F115W} - m_{\rm F322W2}$ CMD with appropriate isochrones suggests that the range in O of M dwarfs is similar to that inferred for red giants (Milone et al. 2023).

Preliminary results from the spectroscopic analysis of NIRSpec data suggest that clear differences are detectable for M dwarfs belonging to different stellar populations. Similarly to what inferred from photometry, the range in O from the spectra is similar the one observed in higher-mass stars (Marino et al. 2023b).

Finally, JWST data for M dwarfs, both the CMD and the spectra, are consistent with the low mass stars sharing the same O variations as the higher mass stars on the RGB, which represents a challenge for any accretion scenario. I conclude by emphasizing that the JWST data will open new exciting perspectives for the investigation of multiple

https://doi.org/10.1017/S1743921323001163 Published online by Cambridge University Press

stellar populations and possibly will provide us the solution for a long-standing enigma of stellar astrophysics.

## References

Baraffe, I., Homeier, D., Allard, F., et al. 2015, *A&A*, 577, A42. doi:10.1051/0004-6361/201425481

Bastian, N., Lamers, H. J. G. L. M., de Mink, S. E., et al. 2013, *MNRAS*, 436, 2398. doi:10.1093/mnras/stt1745

Carretta, E., Bragaglia, A., Gratton, R. G., et al. 2009, *A&A*, 505, 117. doi:10.1051/0004-6361/200912096

D'Antona, F. & Mazzitelli, I. 1994, *ApJ*, 90, 467. doi:10.1086/191867

Decressin, T., Meynet, G., Charbonnel, C., et al. 2007, *A&A*, 464, 1029. doi:10.1051/0004-6361:20066013

de Mink, S. E., Pols, O. R., Langer, N., et al. 2009, *A&A*, 507, L1. doi:10.1051/0004-6361/200913205

Denissenkov, P. A. & Hartwick, F. D. A. 2014, *MNRAS*, 437, L21. doi:10.1093/mnrasl/slt133

Dondoglio, E., Milone, A. P., Renzini, A., et al. 2022, *ApJ*, 927, 207. doi:10.3847/1538-4357/ac5046

Dotter, A., Chaboyer, B., Jevremović, D., et al. 2008, *ApJS*, 178, 89. doi:10.1086/589654

Dotter, A., Ferguson, J. W., Conroy, C., et al. 2015, *MNRAS*, 446, 1641. doi:10.1093/mnras/stu2170

Gieles, M., Charbonnel, C., Krause, M. G. H., et al. 2018, *MNRAS*, 478, 2461. doi:10.1093/mnras/sty1059

Legnardi, M. V., Milone, A. P., Armillotta, L., et al. 2022, *mnras*, 513, 735. doi:10.1093/mnras/stac734

Marino, A. F., Milone, A. P., Renzini, A., et al. 2019a, *MNRAS*, 487, 3815. doi:10.1093/mnras/stz1415

Marino, A. F., Milone, A. P., Sills, A., et al. 2019b, *ApJ*, 887, 91. doi:10.3847/1538-4357/ab53d9

Marino, A. F., et al. 2023a, in preparation

Marino, A. F., et al. 2023b, in preparation

Milone, A. P., Marino, A. F., Cassisi, S., et al. 2012, *ApJL*, 754, L34. doi:10.1088/2041-8205/754/2/L34

Milone, A. P., Marino, A. F., Bedin, L. R., et al. 2014, *MNRAS*, 439, 1588. doi:10.1093/mnras/stu030

Milone, A. P., Marino, A. F., Piotto, G., et al. 2015, *ApJ*, 808, 51. doi:10.1088/0004-637X/808/1/51

Milone, A. P., Piotto, G., Renzini, A., *et al.* 2017, *MNRAS*, 464, 3636

Milone, A. P., Marino, A. F., Bedin, L. R., et al. 2019, *MNRAS*, 484, 4046. doi:10.1093/mnras/stz277

Milone, A. P., Marino, A. F., Dotter, A., et al. 2023, arXiv:2301.10889. doi:10.48550/arXiv.2301.10889

Milone, A. P. & Marino, A. F. 2022, Universe, 8, 359. doi:10.3390/universe8070359

Renzini, A., D'Antona, F., Cassisi, S., et al. 2015, *MNRAS*, 454, 4197. doi:10.1093/mnras/stv2268

Renzini, A., Marino, A. F., & Milone, A. P. 2022, *MNRAS*, 513, 2111. doi:10.1093/mnras/stac973

Ventura, P. & D'Antona, F. 2009, *A&A*, 499, 835. doi:10.1051/0004-6361/200811139